Three-dimensional (3D) information of capturing and reconstructing an object existing in its environment is a big challenge. In this work, we discuss the 3D laser scanning techniques, which can obtain a high density of data points by an accurate and fast method. This work considers the previous developments in this area to propose a developed cost-effective system based on pinhole projection concept and commercial hardware components taking into account the current achieved accuracy. A laser line auto-scanning system was designed to perform close-range 3D reconstructions for home/office objects with high accuracy and resolution. The system changes the laser plane direction with a microcontroller to perform automatic scanning and obtain continuous laser strips for objects' 3D reconstruction. The system parameters were calibrated with Matlab's built-in camera calibration toolbox to find camera focal length and optical center constraints. The pinhole projection equation was defined to optimize the prototype rotating axis equation. The developed 3D environmental laser scanner with pinhole projection proved the system's effectiveness on close-range stationary objects with high resolution and accuracy with a measurement error in the range (0.05–0.25) mm. The 3D point cloud processing of the Matlab computer vision toolbox has been employed to show the 3D object reconstruction and to perform the camera calibration, which improves efficiency and highly simplifies the calibration method. The calibration error is the main error source in the measurements, and the errors of the actual measurement are found to be influenced by several environmental parameters. The presented platform can be equipped with a system of lower power consumption, and compact smaller size

Keywords: three-dimensional laser scanners, visualization, camera calibration, pinhole projection, 3D reconstruction

UDC 528
DOI: 10.15587/1729-4061.2021.227629

DEVELOPMENT OF 3D ENVIRONMENTAL LASER SCANNER USING PINHOLE PROJECTION

Lateef Abd Zaid Qudr
Doctor of Computer Sciences,
Senior Lecturer
Department of Computer
Techniques Engineering
AlSafwa University College
Almamalje str.,
Karbala, Iraq, 56001
E-mail: latifkhder@alsafwa.edu.iq

Received date 15.02.2020
Accepted date 22.03.2021
Published date 20.04.2021

How to Cite: *Qudr, L. A. Z. (2021). Development of 3D environmental laser scanner using pinhole projection. Eastern-European Journal of Enterprise Technologies, 2 (1 (110)), 37–43. doi: https://doi.org/10.15587/1729-4061.2021.227629*

1. Introduction

In order to enhance the implementation of different object designs and human-environment solutions for 3D printing purposes and object regenerations, advanced digital applications can have a considerable impact. The innovation of 3D scanners is important because it can settle the problems that are usually associated with the construction and design of existing objects. It can present better quality, more precise and faster analysis and feature detection for small or large-scale environment surveys [1]. A laser-based 3D scanner is directed to the physical object's under-scan and the beam of the laser is targeted to the object over a grid of points. The position in the 3D space of each scanned point on the object is recognized by determining the laser flight time (scanner-physical objects-scanner). This process results in a «cloud of points» that includes thousands of 3-dimensional space points. This information provides an accurate representation of the scanned object. This data can be transformed into a 3D model. Related researches have proven that the 3D laser scanners can provide effective sensing modality to create an accurate model [2, 3]. Three-dimensional (3D) laser scanners require high resolution to reconstruct an accurate 3D model [4, 5].

Several types of research implemented 3D laser scanner in various applications such as in 3D complex topography with terrestrial applications [6–9], for autonomous driving [10–15], for orthodontic applications [16–18], for industrial and robotics applications [19–23], and in biological applications [24, 25]. In these applications, short-distance cameras and sensors were used to acquire accurate 3D geometrical data of an object. Cameras are commonly utilized as passive sensors while other sensors have relied on light projection or sounds. The 3D environments are sensed with a series of photos acquired from various viewpoints in passive methods. Therefore, the object 3D data will be retrieved with algorithms of stereo matching or image features matching [26, 27]. The accuracy of the restructured model is highly influenced by the visibility environment and needs a textured scene to obtain satisfactory outcomes [1, 28]. The wavelength diversity of projection light and the larger lighting volume will guide to wider absorption and scattering stages. In a 3D scanner environment, scanners with different wavelengths of laser were used in a low absorption environment. Higher luminance with small power is necessary to obtain an accurate and efficient model to identify the object. A motor-based motion generator is essential to cover a large area during the scan with a single laser line.

The main motivation of this work is to develop a 3D scanner to provide a restructured industry model [29], autonomous manipulation [30–32], or 3D printing tasks with high accuracy and low cost [33–35]. Therefore, the system camera, mechanism, and algorithm need to accurately provide geometrical measurements for the object under test, including position, size, shape, etc. Also, the precision of the motion control mechanism is an essential issue in 3D reconstructions.

Therefore, studies that are devoted to 3D laser scanners are relatively complex and costly systems when utilizing in topography with terrestrial applications, autonomous driving, orthodontic applications, biological, industrial, and robotics. In these applications, long and short-distance cameras and sensors were used to acquire accurate 3D geometrical data of an object.

The accuracy of the restructured model is highly influenced by the visibility environment and needs a textured scene to obtain satisfactory outcomes. Higher luminance with small power is necessary to obtain an accurate and efficient model to identify the object. A motor-based motion generator is essential to cover a large area during the scan with a single laser line.

2. Literature review and problem statement

3D laser scanner techniques in a built environment have been discussed in several previous studies. The 3D terrestrial laser scanner for the built environment was presented as a world data model in [36]. This approach used different planes to produce 2D planes, which improves the efficiency and quality of construction projects such as maintenance of buildings, but there is no sufficient information about the system design. The study [37] discussed the application of underwater 3D reconstruction with a laser line auto-scanning system, it employed a galvanometer's rotating axis equation. This work doesn't address a generalized algorithm that can automatically split shape objects with respect to the view field point cloud.

The paper [38] investigated the feasibility of utilizing scanners with handheld structure sensors to create a 3D graphical representation of an object. This work is good for scanning objects with less than 1 m^3 volume. Larger object ability to scan is done by using HDS 3000 by Leica Geosystem [39], but it was with expensive components and complex software. The reasons for it can be objective difficulties connected to the laser source and the costly camera, which makes the corresponding researches unaffordable. An option to overcome the relevant difficulties can be the use of hand-held structure sensors that are inexpensive and accurate solutions [40]. In the study [41], the accuracy of Transport Layer Security (TLS) was assessed by scanning and modeling a room, the work compared the measurement differences with a high-accuracy laser scanner [42]. The study removes the noise and aligned multiple scans with SketchUp 3D modelling software [43]. However, all this allows us to argue that it is appropriate to conduct a study devoted to a cost-effective design with appropriate hardware components and a control algorithm competing with the current structures in the 3D reconstruction accuracy.

3. The aim and objectives of the study

The study aims to build a 3D reconstruction environmental laser scanner for close-range home/office objects with high accuracy and resolution.

The following objectives have been set to achieve the goal:

– to calibrate system parameters with Matlab's built-in camera calibration toolbox to find camera focal length and optical center constraints;

– to develop an algorithm for getting a point cloud for the tested object in its 3D environment;

– to get a mesh representation by defining the pinhole projection equation to optimize the prototype rotating axis equation.

4. Materials and methodology

The methodology includes a design of a 3D reconstruction with an affordable controllable turntable, model scale, camera calibration, and laser line filtering. The system is composed of a stepper motor, C920 Webcam [44], Laser Line diode LASIRIS series (ProPhotonix Limited, Salem, UT, USA), and Arduino controlled turntable. Fig. 1 shows the developed system structure. The experimental measurements have been conducted in different light conditions to also check the effect of the environmental light. The generated mesh representation has been validated by measuring the error as compared with the physical object.

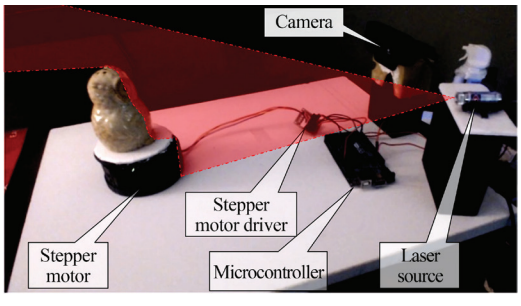

Fig. 1. Developed system setup

A camera and a laser-stepper motor motion module unit were mounted in two independent places and fixed to a base structure to keep its relative position stationary. The distances between the camera, the laser source, and the object were accurately measured after the system was processed and installed. The servomotor can be controlled to rotate in the range of ±20 by a signal ranging between –10 V to +10 V from the D/A of the controller. The laser plane is projected onto the scanned object. The stepper motor controls the laser plane rotating within a certain step angle. The 3D data of the object surface could be obtained based on the computation of the optical information with the pinhole projection equation and triangulation methods. 3D point cloud processing of the Matlab computer vision toolbox has been employed to show the 3D object reconstruction.

4. 1. Stepper motor configuration

The full step sequence of the stepper motor function can be described in Fig. 2.

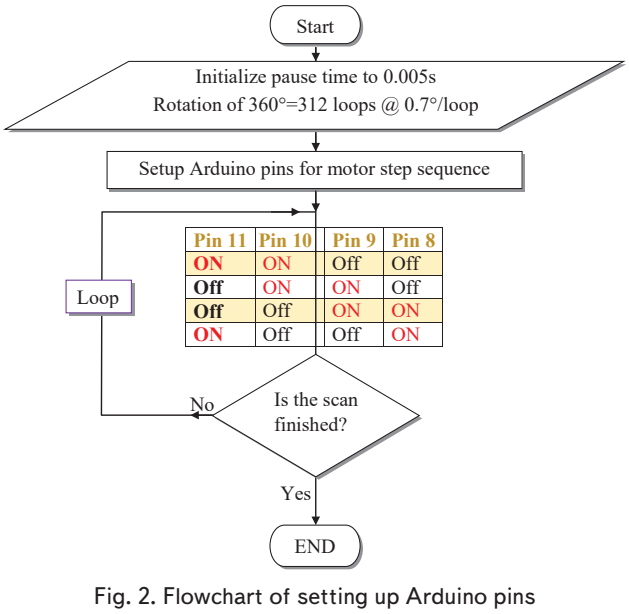

Fig. 2. Flowchart of setting up Arduino pins for motor movement

The steps of controlling the motor of the laser are initialized with 0.005 s pause time and 312 loops at 0.7°/loop equivalent to 360°. The pins (8–11) were used to control the stepper motor movement direction and speed. The scan is stopped when the scan accomplished its limits.

4. 2. Basic pinhole projection equation

Fig. 3 shows a simple pinhole camera description.

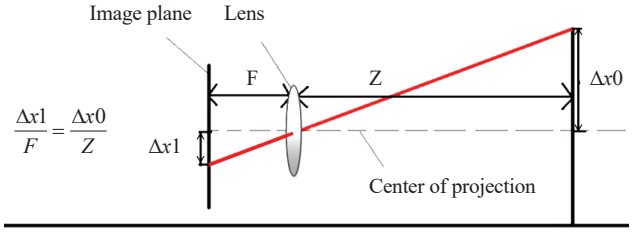

Fig. 3. Pinhole camera description

This work presents a stepper motor-based motion mechanism and the laser plane orientation is changed accurately according to the camera feedback and a controlled algorithm using the pinhole projection principle. The minimal control accuracy for the scanning sector of the stepper motor is 10 μrad, which provides high image resolution and accurate object reconstruction. The outer dimensions of the prototype were 580 m (length)×130 mm (width)×200 mm (height). The system voltage supply was 12 V with an average power consumption of 6.5 W, which makes this design suitable for performing 3D reconstruction tasks of mobile applications.

4. 3. Camera calibration

We've used Matlab's built-in camera calibration toolbox to find camera focal length and optical center at a set resolution. The camera is with 960×720 resolution and got a Focal Length=919 px and optical center [495, 335] with 0.13 px accuracy and each square on the checkerboard plane=13 mm. Photos from the calibration process are shown in Fig. 4, while the description of the camera's optical center, at a normal matrix coordinates of an image Fig. 5, *a*, and translated to camera coordinates Fig. 5, *b*.

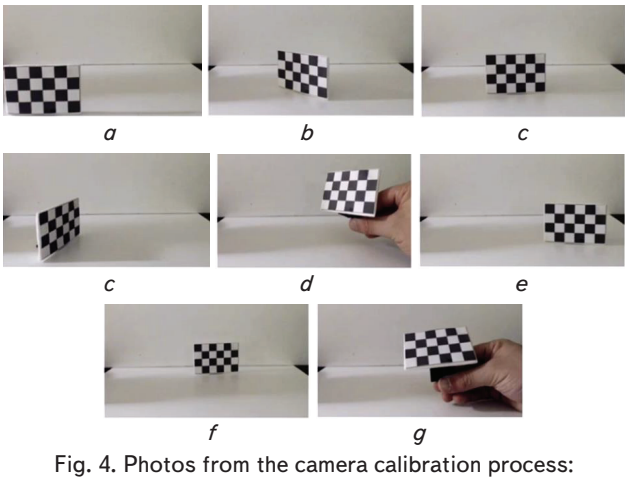

Fig. 4. Photos from the camera calibration process: *a* – left corner and straight face; *b* – centered and sloped face; *c* – centered and straight face; *d* – corner and sloped face; *e* – lifted sloped face; *f* – right corner and straight face; *g* – far centered and straight face; *h* – right corner and sloped face

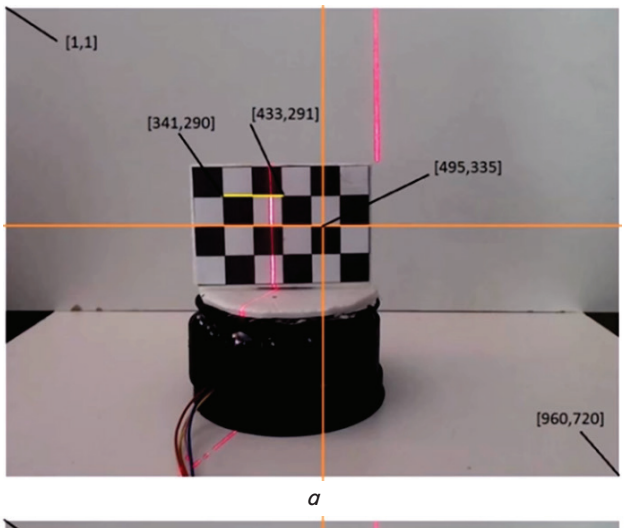

a

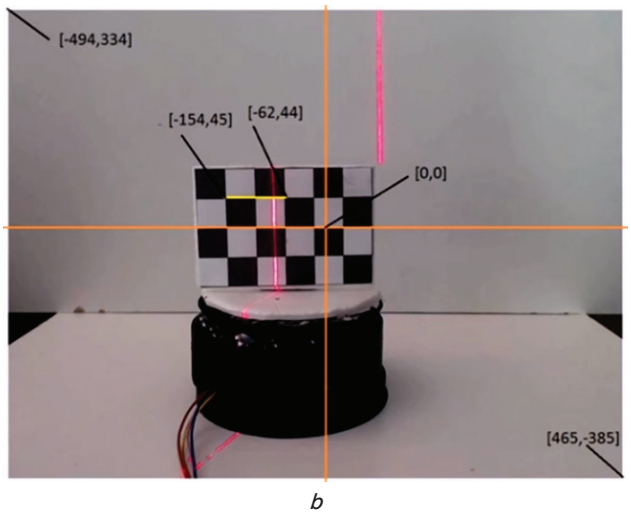

b

Fig. 5. Description of the camera's optical center: *a* – at a normal matrix coordinates of an image; *b* – at translated to camera coordinates

As described above, the basic mathematical pinhole equation is given by:

$$\frac{\Delta x_1}{f} = \frac{\Delta x_o}{Z}.$$

Since we set each square to 13 mm, the length of the yellow line should equal 26. The checkerboard is 260 mm away and the focal length=919 px with the yellow line length=Δx_o:

$$\Delta x_1 = |-154\text{ px} - 62\text{ px}| = 92\text{ px}.$$

By using cross multiplication:

$$\frac{\Delta x_1}{f} = \frac{\Delta x_o}{Z} \rightarrow \frac{Z \cdot \Delta x_1}{f} = \Delta x_o;$$

$$\frac{260\text{ mm} \cdot 92\text{ px}}{919\text{ px}} = \Delta x_o = 26.06\text{ mm}.$$

The geometric model of the camera can be demonstrated as shown in Fig. 6.

Accordingly, to determine the depth from the laser line, we can write the following formula:

$$\frac{\sin(A_o)}{a_o} = \frac{\sin(B_o)}{b} = \frac{\sin(C_o)}{c_o},$$

where C_o is known as the angle of the laser, b is also known that represents the laser distance from the camera. A_o, B_o, c_o, and z_o are given by:

$$A_o = 90 + Pixel\theta;$$

$$B_o = 180 - (A_o + C_o);$$

$$c_o = \frac{\sin\sin(C_o)\cdot b}{\sin\sin(B_o)};$$

$$z_o = c_o \cdot \cos(Pixel\theta).$$

The setting up of the platform parameters, video filter equations, depth mapping, and a viewing point cloud is demonstrated in the flowchart shown in Fig. 7.

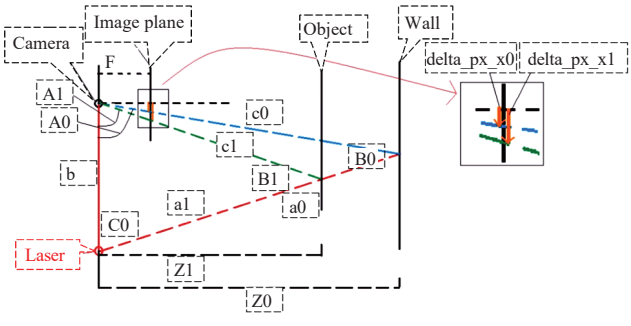

Fig. 6. Geometric model of the camera

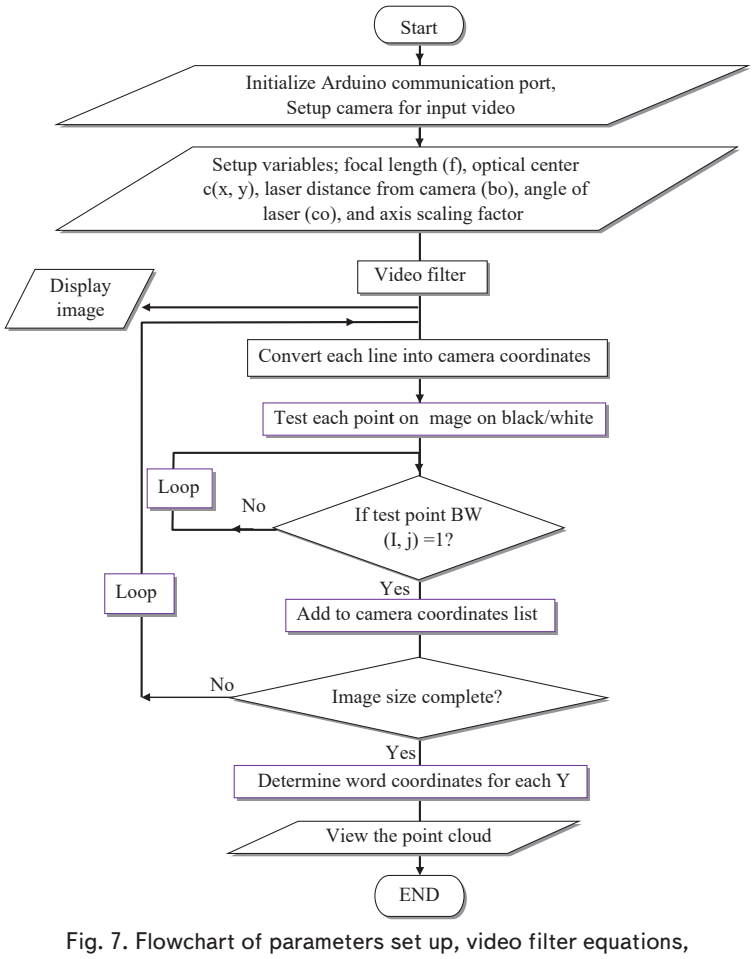

Fig. 7. Flowchart of parameters set up, video filter equations, depth mapping, and viewing point cloud

In order to find Δθ per loop, we mark a point on the turntable, then we run the scan function until 360 degrees is complete. This provides information to figure out how many loops the scan function takes to make a full 360-degree rotation. In the implemented prototype, it was 515 loops so 3.600/515=0.7° per loop.

4. 4. 3D reconstruction

The main program loops the first depth map script and saves the values of each depth map into a variable. However, before each depth map is saved, the points are translated to the world coordinates of the center of the rotating platform then rotated Δθ per loop around the Y-axis. The transformation matrix equation can be given by:

$$\begin{bmatrix} 1 & 0 & 0 & T_x \\ 0 & 1 & 0 & T_y \\ 0 & 0 & 1 & T_z \\ 0 & 0 & 0 & 1 \end{bmatrix} \cdot \begin{bmatrix} x \\ y \\ z \\ 1 \end{bmatrix} =$$

$$= \begin{bmatrix} x+T_x \\ y+T_y \\ z+T_z \\ 1 \end{bmatrix} \rightarrow R_Y = \begin{bmatrix} \cos\theta & 0 & \sin\theta & 0 \\ 0 & 1 & 0 & 0 \\ -\sin\theta & 0 & \cos\theta & 0 \\ 0 & 0 & 0 & 1 \end{bmatrix}.$$

The transformation matrix equation is performed before each mapping step, where the points are translated to the world coordinates of the center of the rotating platform.

5. Results of the proposed 3D laser scanner

5. 1. Camera calibration

The camera and system parameters were calibrated with Matlab's built-in camera calibration toolbox to find camera focal length and optical center constraints. Fig. 8 shows the images of three steps of the developed approach; laser scanning, filtering, depth mapping.

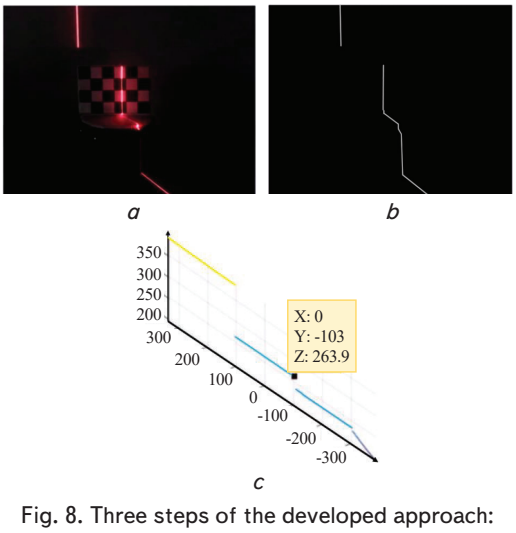

Fig. 8. Three steps of the developed approach: *a* – original image laser scanning, *b* – filtered image; *c* – depth mapping

The images of this figure show a good measurement representation of camera calibration for the 3D environment.

5. 2. Getting a point cloud of the 3D object

The result of carrying out the developed algorithm to get point cloud for the tested object is shown in Fig. 9.

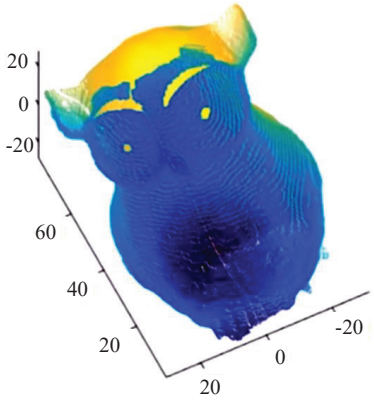

Fig. 9. Point cloud for the tested object

In order to create a 3D printable mesh, it is required to import the point cloud into mesh environment software such as MeshLab, which is free and open-source software [45].

5. 3. 3D printable mesh

The 3D reconstruction of the developed algorithm as a mesh representation for the tested object is shown in Fig. 10.

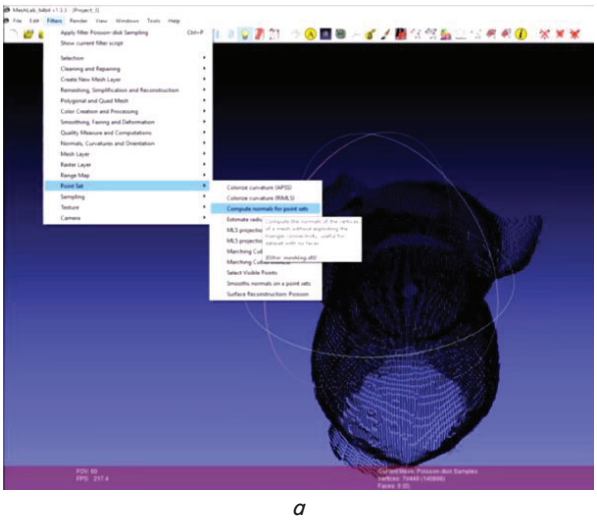

a

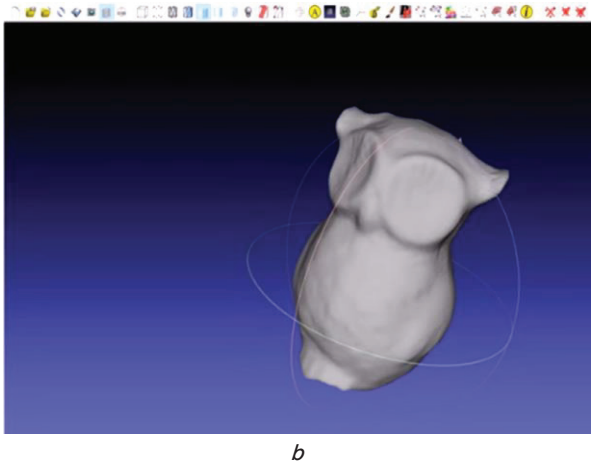

b

Fig. 10. 3D reconstruction of the developed algorithm for the tested object: *a* — mesh figure, *b* — final 3D reconstruction

The generated figures show successful 3D printable mesh and the use of the point cloud into mesh environment software. The developed system proved that this scheme can execute scanning for an object and acquire the 3D point cloud and its outcome validates the accuracy under ideal environments.

6. Discussion of the results of the 3D laser scanner

The results in Fig. 9, 10 show that the developed 3D reconstruction using pinhole formulas and the point cloud can get a successful 3D printable representation. The error was measured in the range (0.05–0.25) mm, which can be considered as accurate 3D reconstruction under this scale of work.

The calibration is carried out with the Matlab camera calibration toolbox, which improves efficiency and highly simplifies the calibration method. The calibration error is the main error source in the measurements, and the errors of the actual measurement are found to be influenced by several environmental parameters.

With the environmental conditions, the reconstructed image is influenced by various lighting and caused by different contrast. With laser and camera parameters, the contrast, gain, offset of the camera, and laser intensity parameters all must be consistent during the scan. These parameters should be optimized to improve the reconstruction accuracy and quality. With the angle between the laser and the camera, when this angle becomes large, the coverage of the scan is also increased and the platform gets compact but this angle needs to be automatically adjusted to fit the scanned object width. This process is done by detecting that there is no intersection with any object except the back wall. Finally, the light scattering is growing, the reconstructed image of an object becomes inaccurate, which may require a laser source with a higher power.

Thanks to which particular features of the proposed solutions, the advantages of the proposed prototype are simple in its hardware components and software with easy implemented control algorithm, and it was also inexpensive as the total cost of the system components is approximately 28 USD, which is less expense and complexity than other current related studies.

The close-range stationary objects were the limitation when applying this approach in the real world. Therefore, more investigation in terms of laser power, laser scanning resolution, and feed-back control actuator is recommended to develop this system to expand its applications.

7. Conclusions

1. The presented calibration of system parameters using Matlab's built-in camera calibration toolbox can be directly applied to find camera focal length and optical center constraints, which consequently reduces the computation cost, and components cost to about 28 USD.

2. The developed 3D environmental laser scanner with pinhole projection proved the system's effectiveness on close-range stationary objects with high resolution and accuracy with a measurement error in the range (0.05–0.25) mm.

3. The developed approach obtained a mesh representation by defining the pinhole projection equation to optimize the prototype rotating axis equation. The system is able to measure a closer distance (140 mm) with an accuracy of (32 μm).

References

1. Arayici, Y., Hamilton, A., Gamito, P., Albergaria, G. (2004). The Scope in the INTELCITIES Project for the Use of the 3D Laser Scanner. Proceedings of the Fourth International Conference on Engineering Computational Technology. doi: https://doi.org/10.4203/ccp.80.51
2. Huber, D. F. (2002). Automatic three-dimensional modeling from reality. CMU-RI-TR-02-35. The Robotics Institute, 201. Available at: https://www.ri.cmu.edu/pub_files/pub3/huber_daniel_2002_1/huber_daniel_2002_1.pdf
3. Bernardini, F., Rushmeier, H. E. (2000). Strategies for registering range images from unknown camera positions. Three-Dimensional Image Capture and Applications III. doi: https://doi.org/10.1117/12.380042
4. Chibane, J., Alldieck, T., Pons-Moll, G. (2020). Implicit Functions in Feature Space for 3D Shape Reconstruction and Completion. 2020 IEEE/CVF Conference on Computer Vision and Pattern Recognition (CVPR). doi: https://doi.org/10.1109/cvpr42600.2020.00700
5. Biffi, C., Cerrolaza, J. J., Tarroni, G., de Marvao, A., Cook, S. A., O'Regan, D. P., Rueckert, D. (2019). 3D High-Resolution Cardiac Segmentation Reconstruction From 2D Views Using Conditional Variational Autoencoders. 2019 IEEE 16th International Symposium on Biomedical Imaging (ISBI 2019). doi: https://doi.org/10.1109/isbi.2019.8759328
6. Lague, D., Brodu, N., Leroux, J. (2013). Accurate 3D comparison of complex topography with terrestrial laser scanner: Application to the Rangitikei canyon (N-Z). ISPRS Journal of Photogrammetry and Remote Sensing, 82, 10–26. doi: https://doi.org/10.1016/j.isprsjprs.2013.04.009
7. Guisado-Pintado, E., Jackson, D. W. T., Rogers, D. (2019). 3D mapping efficacy of a drone and terrestrial laser scanner over a temperate beach-dune zone. Geomorphology, 328, 157–172. doi: https://doi.org/10.1016/j.geomorph.2018.12.013
8. Aicardi, I., Dabove, P., Lingua, A., Piras, M. (2017). Integration between TLS and UAV photogrammetry techniques for forestry applications. iForest – Biogeosciences and Forestry, 10 (1), 41–47. doi: https://doi.org/10.3832/ifor1780-009
9. Biasion, A., Bornaz, L., Rinaudo, F. (2005). Laser Scanning Applications on Disaster Management. Geo-Information for Disaster Management, 19–33. doi: https://doi.org/10.1007/3-540-27468-5_2
10. Zhang, J., Singh, S. (2016). Low-drift and real-time lidar odometry and mapping. Autonomous Robots, 41 (2), 401–416. doi: https://doi.org/10.1007/s10514-016-9548-2
11. Chen, Y., Wang, J., Li, J., Lu, C., Luo, Z., Xue, H., Wang, C. (2018). LiDAR-Video Driving Dataset: Learning Driving Policies Effectively. 2018 IEEE/CVF Conference on Computer Vision and Pattern Recognition. doi: https://doi.org/10.1109/cvpr.2018.00615
12. Krüsi, P., Furgale, P., Bosse, M., Siegwart, R. (2016). Driving on Point Clouds: Motion Planning, Trajectory Optimization, and Terrain Assessment in Generic Nonplanar Environments. Journal of Field Robotics, 34 (5), 940–984. doi: https://doi.org/10.1002/rob.21700
13. Huang, X., Cheng, X., Geng, Q., Cao, B., Zhou, D., Wang, P. et. al. (2018). The ApolloScape Dataset for Autonomous Driving. 2018 IEEE/CVF Conference on Computer Vision and Pattern Recognition Workshops (CVPRW). doi: https://doi.org/10.1109/cvprw.2018.00141
14. Hu, H., Zhao, T., Wang, Q., Gao, F., He, L. (2020). R-CNN Based 3D Object Detection for Autonomous Driving. CICTP 2020. doi: https://doi.org/10.1061/9780784483053.077
15. Li, B., Ouyang, W., Sheng, L., Zeng, X., Wang, X. (2019). GS3D: An Efficient 3D Object Detection Framework for Autonomous Driving. 2019 IEEE/CVF Conference on Computer Vision and Pattern Recognition (CVPR). doi: https://doi.org/10.1109/cvpr.2019.00111
16. Wang, X., Jiang, M., Zhou, Z., Gou, J., Hui, D. (2017). 3D printing of polymer matrix composites: A review and prospective. Composites Part B: Engineering, 110, 442–458. doi: https://doi.org/10.1016/j.compositesb.2016.11.034
17. Zaharia, C., Gabor, A.-G., Gavrilovici, A., Stan, A. T., Idorasi, L., Sinescu, C., Negruțiu, M.-L. (2017). Digital Dentistry – 3D Printing Applications. Journal of Interdisciplinary Medicine, 2 (1), 50–53. doi: https://doi.org/10.1515/jim-2017-0032
18. Thrun, S., Burgard, W., Fox, D. (2000). A real-time algorithm for mobile robot mapping with applications to multi-robot and 3D mapping. Proceedings 2000 ICRA. Millennium Conference. IEEE International Conference on Robotics and Automation. Symposia Proceedings (Cat. No.00CH37065). doi: https://doi.org/10.1109/robot.2000.844077
19. Skotheim, O., Lind, M., Ystgaard, P., Fjerdingen, S. A. (2012). A flexible 3D object localization system for industrial part handling. 2012 IEEE/RSJ International Conference on Intelligent Robots and Systems. doi: https://doi.org/10.1109/iros.2012.6385508
20. Lindner, L., Sergiyenko, O., Rodríguez-Quiñonez, J. C., Rivas-Lopez, M., Hernandez-Balbuena, D., Flores-Fuentes, W. et. al. (2016). Mobile robot vision system using continuous laser scanning for industrial application. Industrial Robot: An International Journal, 43 (4), 360–369. doi: https://doi.org/10.1108/ir-01-2016-0048
21. Kriegel, S., Bodenmuller, T., Suppa, M., Hirzinger, G. (2011). A surface-based Next-Best-View approach for automated 3D model completion of unknown objects. 2011 IEEE International Conference on Robotics and Automation. doi: https://doi.org/10.1109/icra.2011.5979947
22. Blais, F., Picard, M., Godin, G. (2004). Accurate 3D acquisition of freely moving objects. Proceedings. 2nd International Symposium on 3D Data Processing, Visualization and Transmission, 2004. 3DPVT 2004. doi: https://doi.org/10.1109/tdpvt.2004.1335269
23. Zhongdong, Y., Peng, W., Xiaohui, L., Changku, S. (2014). 3D laser scanner system using high dynamic range imaging. Optics and Lasers in Engineering, 54, 31–41. doi: https://doi.org/10.1016/j.optlaseng.2013.09.003

24. Tocheri, M. W. (2009). Laser Scanning: 3D Analysis of Biological Surfaces. Advanced Imaging in Biology and Medicine, 85–101. doi: https://doi.org/10.1007/978-3-540-68993-5_4
25. Hennessy, R. J., Kinsella, A., Waddington, J. L. (2002). 3D laser surface scanning and geometric morphometric analysis of craniofacial shape as an index of cerebro-craniofacial morphogenesis: initial application to sexual dimorphism. Biological Psychiatry, 51 (6), 507–514. doi: https://doi.org/10.1016/s0006-3223(01)01327-0
26. Leone, A., Diraco, G., Distante, C. (2007). Stereoscopic System for 3-D Seabed Mosaic Reconstruction. 2007 IEEE International Conference on Image Processing. doi: https://doi.org/10.1109/icip.2007.4379212
27. Drap, P., Seinturier, J., Scaradozzi, D., Gambogi, P., Long, L., Gauch, F. (2007). Photogrammetry for virtual exploration of underwater archeological sites. XXI International CIPA Symposium. Athens.
28. Bianco, G., Gallo, A., Bruno, F., Muzzupappa, M. (2013). A Comparative Analysis between Active and Passive Techniques for Underwater 3D Reconstruction of Close-Range Objects. Sensors, 13 (8), 11007–11031. doi: https://doi.org/10.3390/s130811007
29. Wang, B., Jiang, L., Li, J. W., Cai, H. G., Liu, H. (2005). Grasping unknown objects based on 3d model reconstruction. Proceedings, 2005 IEEE/ASME International Conference on Advanced Intelligent Mechatronics. doi: https://doi.org/10.1109/aim.2005.1511025
30. Rusu, R. B., Blodow, N., Marton, Z. C., Beetz, M. (2009). Close-range scene segmentation and reconstruction of 3D point cloud maps for mobile manipulation in domestic environments. 2009 IEEE/RSJ International Conference on Intelligent Robots and Systems. doi: https://doi.org/10.1109/iros.2009.5354683
31. Rusu, R. B. (2010). Semantic 3D Object Maps for Everyday Manipulation in Human Living Environments. KI – Künstliche Intelligenz, 24 (4), 345–348. doi: https://doi.org/10.1007/s13218-010-0059-6
32. Beall, C., Lawrence, B. J., Ila, V., Dellaert, F. (2010). 3D reconstruction of underwater structures. 2010 IEEE/RSJ International Conference on Intelligent Robots and Systems. doi: https://doi.org/10.1109/iros.2010.5649213
33. Straub, J., Kerlin, S. (2014). Development of a Large, Low-Cost, Instant 3D Scanner. Technologies, 2 (2), 76–95. doi: https://doi.org/10.3390/technologies2020076
34. Louvrier, A., Marty, P., Barrabé, A., Euvrard, E., Chatelain, B., Weber, E., Meyer, C. (2017). How useful is 3D printing in maxillofacial surgery? Journal of Stomatology, Oral and Maxillofacial Surgery, 118 (4), 206–212. doi: https://doi.org/10.1016/j.jormas.2017.07.002
35. Birtchnell, T., Hoyle, W., Birtchnell, T., Hoyle, W. (2016). What is 3D Printing? The definitive guide. 3D Print Dev Glob South.
36. Arayici, Y. (2007). An approach for real world data modelling with the 3D terrestrial laser scanner for built environment. Automation in Construction, 16 (6), 816–829. doi: https://doi.org/10.1016/j.autcon.2007.02.008
37. Chi, S., Xie, Z., Chen, W. (2016). A Laser Line Auto-Scanning System for Underwater 3D Reconstruction. Sensors, 16 (9), 1534. doi: https://doi.org/10.3390/s16091534
38. Allegra, D., Gallo, G., Inzerillo, L., Lombardo, M., Milotta, F. L. M., Santagati, C. et. al. (2016). Low cost handheld 3D scanning for architectural elements acquisition. STAG: Smart Tools and Apps in computer Graphics. doi: https://dx.doi.org/10.2312/stag.20161372
39. Reshetyuk, Y. (2006). Calibration of terrestrial laser scanners Callidus 1.1, Leica HDS 3000 and Leica HDS 2500. Survey Review, 38 (302), 703–713. doi: https://doi.org/10.1179/sre.2006.38.302.703
40. Bauwens, S., Bartholomeus, H., Calders, K., Lejeune, P. (2016). Forest Inventory with Terrestrial LiDAR: A Comparison of Static and Hand-Held Mobile Laser Scanning. Forests, 7 (12), 127. doi: https://doi.org/10.3390/f7060127
41. Lee, S. Y., Majid, Z., Setan, H. (2013). 3D data acquisition for indoor assets using terrestrial laser scanning. ISPRS Annals of Photogrammetry, Remote Sensing and Spatial Information Sciences, II-2/W1, 221–226. doi: https://doi.org/10.5194/isprsannals-ii-2-w1-221-2013
42. Abbas, M. A., Setan, H., Majid, Z., Chong, A. K., Idris, K. M., Aspuri, A. (2013). Calibration and Accuracy Assessment of Leica ScanStation C10 Terrestrial Laser Scanner. Developments in Multidimensional Spatial Data Models, 33–47. doi: https://doi.org/10.1007/978-3-642-36379-5_3
43. Wolk, R. M. (2008). Utilizing Google Earth and Google Sketchup to visualize wind farms. 2008 IEEE International Symposium on Technology and Society. doi: https://doi.org/10.1109/istas.2008.4559793
44. LOGITECH® HD PRO WEBCAM C920. Available at: https://docs.rs-online.com/97f0/A700000006917072.pdf
45. MeshLab. Available at: https://www.meshlab.net/